Advances in Science and Technology Research Journal

Advances in Science and Technology Research Journal 2023, 17(6), 27–38
https://doi.org/10.12913/22998624/172981
ISSN 2299-8624, License CC-BY 4.0

Received: 2023.09.14
Accepted: 2023.10.27
Published: 2023.11.21

Influence of Surface Laser Treatment on Mechanical Properties and Residual Stresses of Titanium and its Alloys

Magdalena Jażdżewska[1*], Beata Majkowska-Marzec[1], Roman Ostrowski[2], Jean-Marc Olive[3]

[1] Department of Biomaterials Technology, Institute of Manufacturing and Materials Technology, Faculty of Mechanical Engineering and Ship Technology, Gdansk University of Technology, 80-233 Gdansk, Poland
[2] Institute of Optoelectronics, Military University of Technology, Warszawa, Poland
[3] CNRS, Institute of Mechanics and Engineering, University of Bordeaux, 33400 Talence, France
* Corresponding author's e-mail: magdalena.jazdzewska@pg.edu.pl

ABSTRACT

Surface modification of the titanium and its alloys used in implantology with a long-pulse laser can change the surface topography, but it also leads to changes in the stress sign and magnitude in the resulting subsurface layer. The presented research was aimed at evaluating the state of stress after laser remelting with the Nd:YAG laser of pre-etched titanium alloys Ti6Al4V and Ti13Nb13Zr and pure titanium.The obtained surface layers were characterized using scanning electron microscopy (SEM), X-ray diffraction (XRD), optical profilography, and nanoindentation studies. Based on the results obtained after the nanoindentation tests, the character of the stresses generated in the melted layers was calculated and determined. Laser processing resulted in surface layer thicknesses between 191–320 µm and surface roughness Ra between 2.89–5.40 µm. Laser processing caused increasing hardness, and its highest value was observed for the titanium alloy Ti13Nb13Zr – 5.18 GPa.The tensile stressesappeared following laser treatment andincreased with elevating laser power up to the highest value for titanium.

Keywords: titanium, laser treatment, residual stresses, mechanical properties, roughness.

INTRODUCTION

Titanium and its alloys as lightweight metals of high relative mechanical strength and fatigue limit, corrosion resistance, and outstanding biocompatibility at moderate costs are found in different branches of modern industry, as materials for aircraft [1, 2], marine applications [3], military equipment, industrial-technological systems, automotive parts, farming fitting, sporting goods, and biomedical engineering [4, 5]. In particular, in medicine, titanium-based alloys are mostly applied to fabricate long-term implants, or their parts, such as the dental, hip joint, knee, and other implants, load-bearing applications [6, 7]. The most important value of these materials for medicine is in their high strength-to-density ratio, remarkable corrosion resistance, small elastic modulus compared to various metallic biomaterials, and excellent biocompatibility. However, titanium biomaterials have several disadvantages such as low hardness, insufficient friction resistance, and low bioactivity. Therefore, not only the search for new titanium alloys, but first of all numerous surface modifications are developed to model the surface topography, morphology, and chemical composition. Such modifications can be divided into several groups such as mechanical, chemical, physical, and electrochemical techniques [8]. All these techniques can be also classified as methods based on (i) the transformation of surface layers by mechanical or heat energy, and (ii) the deposition of coatings.

The transformation of surface layers can be based on the delivery of mechanical energy by,

e.g., grinding which can change the microstructure, and increase the density of dislocations and mechanical strength and hardness [9]. Heat transformation can enhance the surface remelting of solids, diffusion of elements, etc. Such energy is most frequently delivered by laser beam, much less often by electron beam. Another possibility of surface modification comprises the deposition of coatings by different techniques, mainly air and vacuum plasma spraying, electrocathodic and electrophoretic deposition, and physical methods such as PVD (plasma vapor deposition) and CVD (chemical vapor deposition) [8, 10–12].

Among those methods, laser-assisted techniques are investigated, developed, and applied for surface modifications of titanium and its alloys. The most popular is the laser shot peening method used for introducing compressive stresses, increasing hardness, and roughness for mainly an improvement of fatigue resistance of Ti6Al4V alloy [13–15]. The laser cladding is applied to a variety ofmaterials, and in the case of the above alloy, the TiB – Ti_2B titanium-based matrix composite coating was obtained by the laser cladding technique [16]. The laser beam is also used for laser marking, coloring [17], and cleaning [18] of titanium materials.A new process to manufacture thin metal foils using laser shock waves was developed [19]. In addition, it is worth mentioning additive manufacturing, the selective laser melting of parts of Ti alloys that can create scaffolds with designed structures, proposed for bone reconstruction [20].

An intensively studied technique for modifying titanium and its alloys involves the straight impact of a laser beam focused on the surface, which allows for the desired change in the surface topography. Under the action of the laser fluency and local temperature increase, the surface can significantly change its topography and morphology, depending on the fluence (energy density), pulse power, repetition rate, and scan rate [21]. The surface layer becomes more defective due to the appearance of ripples, micro columns, nanopillars [22, 23], micro protrusions and grooves [24], nanocavities [25], cavities [26], and crevices and cracks [27]. The presence of oxygen in the vicinity of the processing zone causes an increase in its content in the surface layer, and often the transformation of titanium and Ti_2O_3 into rutile and anatase dioxide [28]. All these methods may result in enhanced hardness and mechanical strength of the surface layer, increased hydrophilicity, biocompatibility, osteointegration, bioactivity, and sometimes bacteria-killing rate [22, 23, 29–32] as discussed below.

Regarding the mechanical properties of the laser-modified surface, the hardness, strength, and elastic modulus were observed to increase, likely following the melting of the surface layer and its fast recrystallization [26, 33, 34]. The nanoindentation test did not show any relation between mechanical behavior and wear resistance [35].

The femtosecond laser treatment increased hydrophilicity [24] or even introduced superhydrophilicity [28]. The contact angle decreased with increasing laser fluence [27]. The appearance of extremely low contact angles was also observed after laser irradiation followed by additional chemical treatment in H_2O_2 and long exposure to air, presumably due to selective adsorption of some organic species from the atmosphere [36]. The nanosecond laser influence on previously nitride titanium also improved wettability [37]. The observed effects can be described as caused by a substantially developed surface. Corrosion behavior was positively related to laser treatment [37] even if such studies are infrequent.

Biological properties were the most often improved after laser treatment of titanium. Bioactivity, determined as the deposition rate of apatite in phosphate solutions, was enhanced following the fiber laser treatment [38]. The laser-modified surface showed bioactivity observed as proliferation and differentiation of cells [26], and easier protein-absorption process [39]. Osseointegration was measured for titanium laser-treated implants, by the strength of the implant-bone connection [21] and of the implant-bone contact area [26], and showed positive effects. No torque after osseointegration appeared after laser-enhanced modification of the titanium alloy [40]. The antibacterial property was observed for femtosecond laser-irradiated titanium resulting from an absence of adhesion of *Porphyromonas* and *Streptococcus* bacteria [41]. It is also worth noting that after laser processing, the occurrence of surface compressive or tensile residual stresses was observed [21, 28, 42, 43].

Previous studies demonstrate that laser treatment can efficiently influence several surface titanium properties.The main implications are grain size reduction until the appearance of a nanostructure, the presence of non-equilibrium intermetallic compounds and oxides after melting the near-surface layer, and rapid cooling, as

Table 1. Chemical composition of tested materials (according to the manufacturers` certificates)

Material	Al	V	C	Fe	O	N	H	Nb	Zr	Ti
Ti	-	-	0.01	0.18	0.34	0.01	-	-	-	balance
Ti6Al4V	6.09	3.21	0.01	0.16	0.185	0.005	0.003	-	-	balance
Ti13Nb13Zr	-	-	0.035	0.085	0.078	0.019	0.055	13.18	13.49	balance

well as the growth of residual stress of different signs in the remelted zone. The research presented here, which is a continuation of the author's earlier work [44], focuses on further determining the influence of the surface rearrangement of the titanium sample, additionally etched in this work, determined by the laser power on the mechanical behavior of the surface and the magnitude of residual stresses.

EXPERIMENTAL METHODS

Samples made of Ti grade 2 (delivered by EkspresStal, Luboń, Poland) and of Ti6Al4V – Ti6.4 (delivered by TIMET, Birmingham, UK) and Ti13Zr13Nb - Ti13.13 (delivered by SeaBird Materials Co., Baoji, China) alloys were used for the research. The samples had dimensions of 10x10x4 mm. Sample preparation involved grinding materials on grinding–polishing equipment (Saphir 330 type, ATM GmbH, Mammelzen, Germany) using sandpapers up to 800 grit and etching the samples in 3% hydrofluoric acid.

Laser processing, consisting of remelting the surface of titanium and its alloy samples, was carried out using a pulse Nd:YAG laser (Trulaser Station 5004 type, TRUMPF, Dizingen, Germany). The treatment was carried out for two laser beam power levels of 4500 or 3000 W and a pulse duration of 1 ms. For given repetition rates of 25 s^{-1}, beam sizeof 1 mm, and scanning rateof 1 mm/s, an overlap ratio of 96% was obtained. To prevent oxidation during laser processing (Linde Gaz Poland Sp. z oo, Krakow, Poland), the treatment was performed in an argon atmosphere (Argon 5.0). The sample designations are listed in Table 2.

Table 2. The designations of tested samples

Substrate	Laser beam power (W)	Sample designation
Ti	4500	Ti_4.5
	3000	Ti_3.0
Ti6Al4V	4500	Ti6.4_4.5
	3000	Ti6.4_3.0
Ti13Nb13Zr	4500	Ti13.13_4.5
	3000	Ti13.13_3.0

The SEM (JSM-7800 F type, JEOL Ltd., Tokyo, Japan) was applied to characterize the surface topography thickness of the remelted surface layers. Measurements of the thickness of the laser-modified zone were made on the cross-sections of the melted samples. Samples were ground on papers with a gradation of up to 2000 and polished with diamond paste. Then, the microsections were etched with Kroll's reagent composed of 0.06 mm^3 of HF, 0.12 mm^3 of HNO_3, and 50 mm^3 of distilled water. Afterward, the cross-sections were observed with the SEM, and the remelted area depths were measured.

XRD analyses were performed with an X'PERT-PRO diffractometer (PHILIPS, Almelo, The Netherlands) to determine the phases present in the materials. The Cu Kα radiation at the wavelengths $\lambda K\alpha 1 = 0.15406$ nm and $\lambda K\alpha 2 = 0.15444$ nm and a scan rate of 0.02°/s within a 2Θ range of 10–90° was studied.

The surface roughness was measuredby a JENOPTIK (HommelEtamicWaveline, Jena, Germany) profilographometer. A series of 6 measurements were made for the assumed mapping section at a length of 4 mm and a λc filter 0.8 mm at 0.5 μm intervals. The results obtained during the test were averaged, and the mean roughness value Ra and the standard deviation were calculated for each sample.

Nanoindentation studies were carried out using the NanoTestTM Vantage (MicroMaterials, Wrexham, Great Britain) nanoindenter. 25 measurements were made for each sample. The distance between the indentations was 30 μm. Several measurements were run at a maximum force of 50 mN. Performing one indentation consisted of increasing the force for 20 s from the force equal to zero to the maximum force, then stopping the maximum force for 5 s, in the last step the force decreased from the maximum force to the force equal to zero at a given measurement point. A Berkovich diamond indenter was used for the research, with a pyramidal shape with three walls and a vertex angle of 142.4°. Measurements were

made on reference samples, not subjected to laser treatment, on laser-melted samples to assess the effect of surface modification, and on samples subjected to stress-relief annealing to determine the stress state within the surface layer after laser treatment.

Determination of residual stresses was made based on the average force value at which the adjusted measurement depth was observed in the nanoindentation test. For the maximum force during the measurements equal to 50 mN, a depth of 300 nm was assumed. Residual stresses σ were determined based on the difference in loads (before and after annealing), and the surface area of the Berkovich indentation, according to formula (1) [45].

$$\sigma = \Delta P / A \tag{1}$$

where: ΔP – the difference in load resulting in the same indent depth (for samples before and after annealing);
A – the surface area of the indent.

The values of force at adjusted depth and comparative residual stresses were calculated as means of 25 tests made for each sample, load value, and the presence or not of laser irradiation. Since the standard deviations appeared significantly large, the medians (values for the central position of all values) were also determined.

Thermal treatment was carried out using a vacuum tube furnace PTF 15/75/610 (Protherm Furnaces, Ankara, Turkey) with a power of 7000 W. Treatment parameters were selected based on literature data [46] and are presented in Table 3. The heating rate was the same for all samples and it was 100 °C per hour, slow cooling with an oven was used.

Table 3. Temperature and time of heat treatment of different materials

Material	Temperature (°C)	Time (min)
Ti	600	360
Ti6Al4V	600	360
Ti13Nb13Zr	500	60

RESULTS AND DISCUSSION

SurfaceTopography, Roughness, Phase Composition, and Layer Thickness

Figure 1 illustrates the topography of the surface for all remeltedspecimens. The course of laser paths can be observed, which corresponds to the direction of laser head movement. The observed surface irregularities result from the melting of the top layer of the material and its rapid cooling and, as a result, solidification. In addition, a network of small cracks is visible locally in the examined area. The occurrence of surface roughness is well-known as a laser structuring effect caused by the rapid solidification of the melt, and cracks on the surface are likely due to the appearance of tensile stresses [42]. Both material kind and laser power have no clear influence on these qualitative surface features as all substrates have similar melting/solidification temperatures and similar heat conductivity.

Table 4 presents the roughness results obtained for the tested materials with the calculated means and standard deviations (SD). The highest value of the Ra parameter, equal to 5.40 ±0.64 μm, is observed for the Ti_4.5 sample of technical titanium remelted with the laser power of 4500 W. This value is much higher than for technical titanium without laser treatment (Ti sample), 0.96±0.04 μm, as well as for a sample remelted with a lower power of 3.34±0.05 μm (Ti_3.0 sample). The effect of material composition on the obtained roughness is somewhat unexpected here. All the substrates had similar roughness because they were all prepared in the same way, however, technical titanium shows the highest roughness after treatment at the higher laser power (Ti_4.5 sample), while in the case of lower laser power, the highest roughness is shown by the Ti13Nb13Zr alloy (Ti3.13_3.0 samples). Increasing the laser power causes an important rise inthe roughness of titanium, with only a slight increase in the case of the Ti6Al4V alloy, while for the Ti13Nb13Zr alloy, a negligible decrease in roughness is observed. Therefore, laser modification has a significant effect on the roughness, as the increase in remelting power is accompanied by an increase in surface roughness. In the authors' earlier studies conducted with the same materials at a much lower laser power of 1000 W and without pre-etching the samples, much lower roughness was observed, Ra between 0.38–0.60 μm [44]. Changes in surface roughness following the laser surface modification are due to convection movements during material melting and rapid solidification.The different chemical composition and the appearance of the absence of intermetallic phases can cause local dissolution of

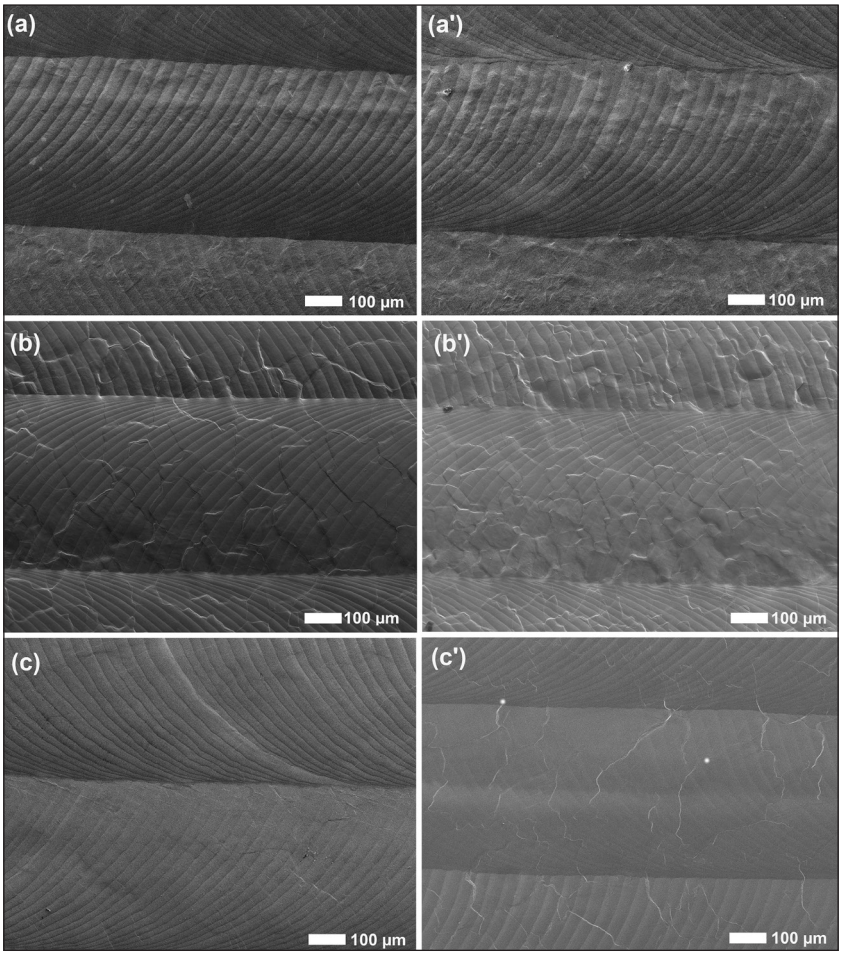

Fig. 1. Surface topographies of samples afterlaser treatment: (a) Ti_4.5,(a') Ti_3.0, (b) Ti6.4_4.5, (b') Ti6.4_3.0, (c) Ti13.13_4.5, (c') Ti13.13_3.0. (SEM)

the last and their much slower precipitation in the quickly cooled surface melted layer. Therefore, titanium can show the highest hardness. More, presumably an absence of intermetallic phasesin titanium results in the smallest grains. In addition, the surface of the samples is more developed, which may lead to an increase in the adsorption of laser beam radiation, a higher temperature on the surface of the samples can be expected, and with solidification, it can lead to greater changes in surface roughness. Such effects are individual and certainly be attributed to the initial microstructure of substrates and the appearance of high local temperatures. In the literature, an increase in surface roughness, and its reduction or no change were already reported, obviously strongly related to the substrate and process parameters such as laser power, scan rate others determining the energy flux and density in time [47].

Table 4. The roughness of the investigated samples

Sample	Roughness ± SD, R_a (µm)
Ti	0.96±0.04
Ti_4.5	5.40±0.64
Ti_3.0	3.34±0.05
Ti6.4	0.31±0.01
Ti6.4_4.5	3.03±0.35
Ti6.4_3.0	2.89±0.32
Ti13.13	0.78±0.12
Ti13.13_4.5	4.28±0.14
Ti13.13_3.0	4.33±0.14

Figure 2 shows the diffraction patterns of all samples after laser treatment. For technical titanium, all peaks are characteristic of the Ti-α phase, and the lack of blurring for the appropriate angle values indicates that the structure has not changed into an amorphous one. In turn, diffraction patterns for the Ti6Al4V alloy after laser treatment at 4500 W (Ti6.4_4.5) and 3000 W (Ti6.4_3.0) do not differ significantly by the following phases: V_7O_3 (for the angle of 64° and 78°), additionally crystalline phases: Ti, $AlTi_3$, Ti_6O for the angle of 35°. In the case of the

Ti13Nb13Zr alloy, there are crystalline phases such as Ti_2Zr (at 34°), NbO_2, Ti, and Ti_2O (at 40°). The spectra of the Ti13Nb13Zr alloy are characterized by a greater blurring of reflections, which corresponds to a smaller grain in the structure [48], in line with previous reports on micro and nanostructure [49]. The sometimes observed coarseness and grain growth [50] do not appear

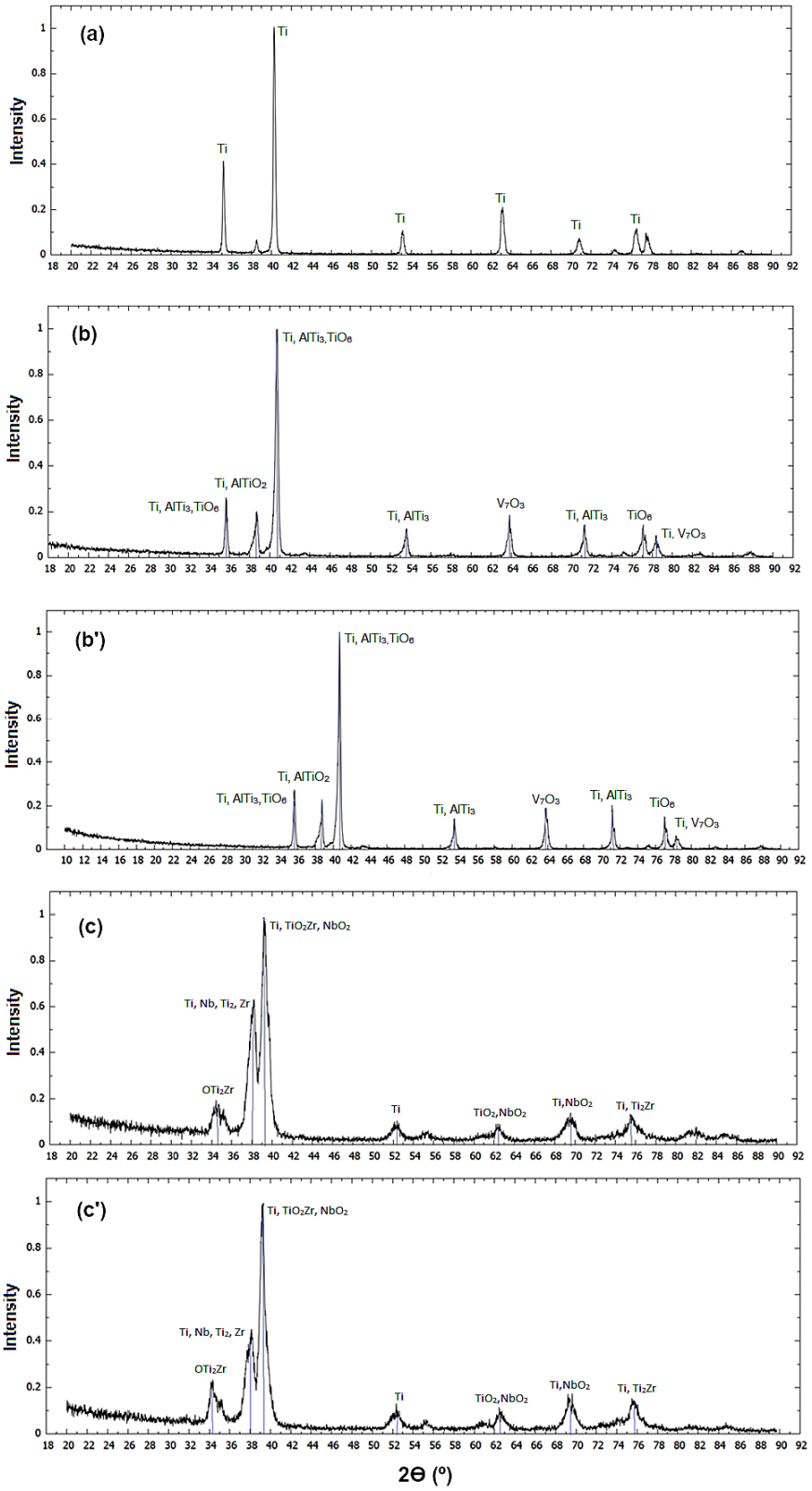

Fig. 2. Phase composition of samples after lasertreatment: – (a) Ti_4.5, (b) Ti6.4_4.5, (b') Ti6.4_3.0, (c) Ti13.13_4.5, (c') Ti13.13_3.0. (XRD)

here, which can be attributed to lower melting temperatures, faster cooling, or both. The observed phase composition is directly related to the laser energy, which results in the decomposition of the intermetallic phases followed by solidification not fast enough to cause the appearance of glass structures in solid solutions. On the contrary, the solidification rate is moderate because some intermetallic phases typical of certain alloys and oxides formed at high temperatures in an oxygen atmosphere may appear [51].

Figure 3 shows cross-sections of laser-treated samples. In the resulting surface layers, a zonal and a coniferous structure can be distinguished. No cracks appear on the cross-sections of the remelted samples. Below the near-surface zone reaching a thickness of about 5 µm, a dendritic structure can be seen. Individual values of the obtained thicknesses of the structure are given in Table 5. It can be then said that the cracks observed on the surface are very shallow so the tensile stresses are present within the very thin subsurface layer. The presence of cracks initiated in the precipitated free zones has already been observed [52, 53].

Mechanical properties

Based on the data obtained from the performance of 25 indentations for the tested materials, the average maximum depth, average hardness, and average Young's modulus were determined, which together with the values of the standard

Table 5. The mean thicknessand the corresponding standard deviation of surface layers after laser treatment

Sample	Thickness ± SD [µm]
Ti_4.5	242.24±29.71
Ti_3.0	208.62±27.95
Ti6.4_4.5	320.26±28.10
Ti6.4_3.0	191.38±14.63
Ti13.13_4.5	290.52±28.36
Ti13.13_3.0	237.50±47.26

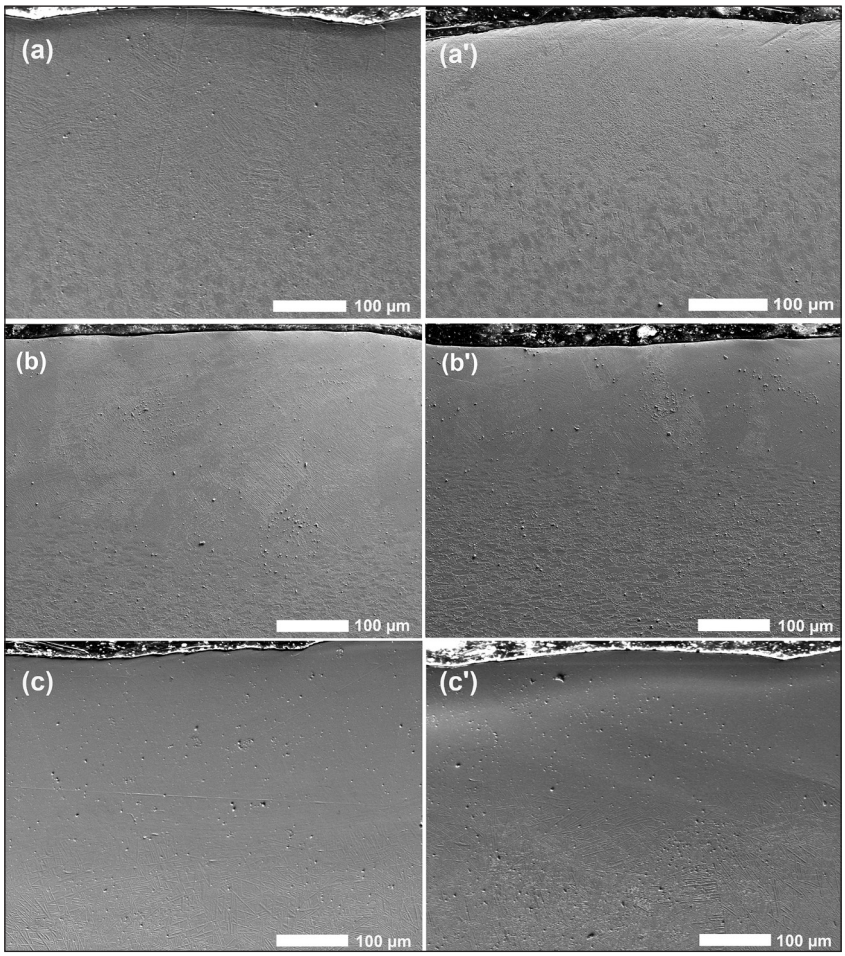

Fig. 3. Cross-sections of laser treated samples: (a) Ti_4.5, (a') Ti_3.0, (b) Ti6.4_4.5, (b') Ti6.4_3.0, (c) Ti13.13_4.5, (c') Ti13.13_3.0. (SEM)

deviations are presented in Table 6. For individual materials, it can be concluded that laser modification undoubtedly increases the hardness of the surface layer. For both technical titanium and the Ti13Nb13Zr alloy, higher hardness was obtained for remeltingat 4500 W than at 3000 W, as shown in three-dimensional hardness maps in Fig. 4. Based on the authors' research to date, it can be concluded that pre-etching of the surface of materials and laser remelting at such high laser power causes a significant decrease in hardness and modulus values: e.g. for 1000 W (samples without etching), for Ti the hardness was 7.2–2.5 GPa and Young's modulus 223.2–68.3 GPa, for Ti6Al4V the hardness was 8.4–2.9 GPa and Young's modulus 199.6–47.9 GPa and, for Ti13Nb13Zr the hardness was 6.7–1.6 GPa and Young's modulus 133.7–27.8 GPa [44]. It may be then concluded that the dominating phenomenon determining the hardness of titanium alloys is the change in the contents of intermetallic phases which decide on hardness in this case. Even if grain size decrease, grain shape change, or possible dislocation multiplication, are less important, they presumably are origins of the laser power effects observed here. However, the relationships between the hardness of the material, its chemical composition, and laser power are complex. Fortitanium, the increasing hardness can be assumed as caused by laser-enhanced localized surface hardening described above. For titanium alloys, an increase or decrease in hardness accompanied by a similar change in elastic modulus can be related to the decomposition of

Table 6. Hardness and Young's modulus determined for different tested titanium materials

Sample	Maximum depth (nm)	Hardness (GPa)	Young's Modulus (GPa)
Ti	1804.71±548.97	0.91±0.61	28.10±15.15
Ti_4.5	870.32±139.20	3.61±1.16	58.77±17.80
Ti_3.0	1227.07±468.36	2.23±1.10	32.56±13.25
Ti6.4	951.05±168.12	2.75±0.91	67.99±17.43
Ti6.4_4.5	1072.87±305.39	3.00±1.49	34.94±13.65
Ti6.4_3.0	935.01±205.81	3.94±2.04	43.64±19.99
Ti13.13	3926.63±631.58	0.15±0.07	9.72±2.04
Ti13.13_4.5	767.29±151.17	5.18±1.93	66.62±24.24
Ti13.13_3.0	877.01±190.47	4.31±1.63	46.25±15.26

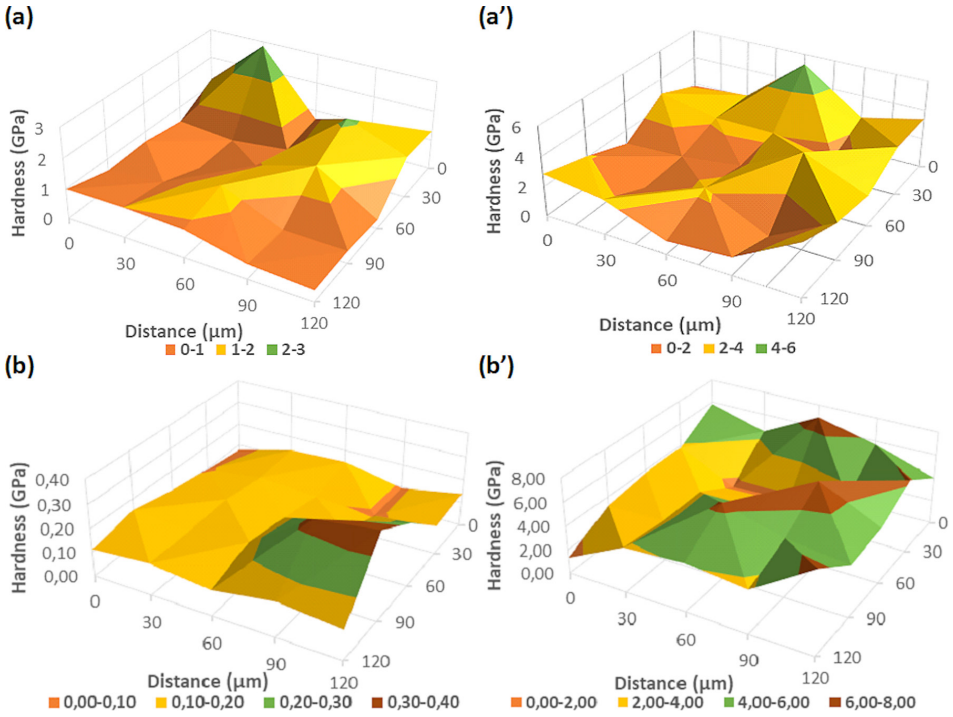

Fig. 4. 3D hardness maps of samples: (a) Ti, (a') Ti_4.5, (b) Ti13.13, (b') Ti13.13_4.5

intermetallic phases and reprecipitation during cooling. However, standard deviations are large and hence the differences between mechanical properties related to different laser energies can be speculative. Nevertheless, the obtained results prove that the laser treatment according to the procedure used herein the laser power range from 3 to 4.5 kW is credible for improvingthe mechanical behavior of the melted zone of all titanium materials.Moreover, Ti13Nb13Zr alloy seems to be the best candidate for the production of surface-hardened titanium material.A similar hardness increase following laser treatment has already been observed [54–56].

To calculate the stress values at the same indent depths, the differences in the means of the forces which have caused the same indent depth, for the samples before and after annealing, were taken into account. The appropriate values of differences between the loading force and the forces calculated at a depth of 300 nm, before and after stress relieving, are presented in Table 7. Besides, the medians for each of these groups are also shown in Table 8. Residual stresses of the substrates and laser-treated specimens were found for a measurement depth of 300 nm and an indentation area of 2.2041 nm^2. All residual stresses are tensile stresses, as indicated by a positive (+) sign.

Tensile stresses occur in all materials after surface remelting with the use of thelong-pulseNd:YAG laser, as in the authors' previous research [43, 44]. Using a laser power of 1000 W for Ti and Ti13.13 samples, much lower stress values were observed, respectively 3.42 and 4.96 GPa [44]. Generally, surface residual compressive or tensile stresses are observed after laser treatment [21, 28, 42, 43]. The tensile stresses observed here are undesired because they can cause cracks initiation and propagation. On the other side, in our experiments thisphenomenon was negligible, so the observed level of stress can be considered harmless. The increasing laser power causesan increase in temperature gradient, which may explain the higher stress values, even if for Ti6Al4V alloy this difference is within the limits of an experimental error. The chemical composition of the titanium material has a scarce effect on the residual stress.

CONCLUSIONS

Among many potential applications of laser sources for the manufacturing and modification of the properties of engineering materials, including cleaning, joining, cladding and cutting [57-59], remelting of metal surfaces plays a special role.

The effect of laser power on surface topography, mechanical behavior, and residual stress level is complex and depends on the type of alloy, i.e., its chemical and phase surface composition. This behavior can be explained by several processes occurring during laser treatment, the finalphase of which is the rapid cooling of the remelted layer. Such processes include solid-to-liquid transition, dissolution of intermetallic phases in Ti alloys, diffusion of elements in the molten layer, liquid-to-solid transition, an appearance of micro and possibly nanostructures, coarseness, and grain growth, presumed appearance of fresh dislocations and vacancies, formation of tensile

Table 7. Differences between superimposed and residual force values after annealing and resulting residual stress values for various laser-treated alloys (means and standard deviations are presented)

Sample	Means of differences of forces at the assumed depth (mN)	Mean resultant stress value (GPa)
Ti	9.90±7.08	4.49±3.21
Ti_4.5	18.60±7.39	8.44±3.35
Ti_3.0	16.21±5.32	7.35±2.41
Ti6.4	10.00±12.94	4.54±5.87
Ti6.4_4.5	13.21±1.14	6.42±0.70
Ti6.4_3.0	12.82±8.29	5.73±3.87
Ti13.13	0.14±0.96	0.06±0.43
Ti13.13_4.5	17.04±6.21	7.74±2.15
Ti13.13_3.0	11.29±2.05	5.12±0.93

Table 8. Medians for differences between superimposed and residual force values after annealing and resulting residual stress values for various laser-treated alloys

Sample	Median of forces at the assumed depth (mN)	Median of resultant stress value (GPa)
Ti	9.34	4.24
Ti_4.5	18.80	8.53
Ti_3.0	10.35	4.69
Ti6.4	2.08	0.95
Ti6.4_4.5	14.21	6.45
Ti6.4_3.0	15.38	6.98
Ti13.13	0.18	0.08
Ti13.13_4.5	19.66	8.92
Ti13.13_3.0	11.60	5.26

mechanical stresses, occurrence of short and shallow cracks.

The type of alloy is important for the final microstructure, topography determined by roughness, hardness, Young`s elastic modulus, and residual stress values, with no further annealing. In particular, hardness and elastic modulus are somewhat higher for Ti alloys due to the precipitation of several Ti intermetallic phases. The differences between all materials are not very significant due to the large amount of titanium in each of them,which determines the properties, and presumably the presence of only small, nano, and microparticles of intermetallic phases in rapidly cooled Ti alloys.

The most suitable laser melting parameters should be determined by roughness, hardness, Young`s modulus, and residual stresses. On this basis, both Ti alloys remelted at 3 kW laser power, can be recommended as the most suitable candidates for such surface modification.

Acknowledgements

We wish to express our gratitude to Professor Andrzej Zieliński for his evaluation of the manuscript and important comments.

The authors also would like to thank the students M. Zielecka and M. Szewc and the employees of Gdansk University of Technology, A. Laska, M. Bartmański, G. Gajowiec, and A. Mielewczyk-Gryń for their technical assistance in some of the tests.

REFERENCES

1. Wu Z., Kou H., Chen N., Xi Z., J. Fan, Tang B., Li J. Recent developments in cold dwell fatigue of titanium alloys for aero-engine applications: a review, Journal of Materials Research and Technology. 20 (2022) 469–484.
2. Zhao Q., Sun Q., Xin S., Chen Y.,Wu C., Wang H., Xu J., Wan M., Zeng W., Zhao Y. High-strength titanium alloys for aerospace engineering applications: A review on melting-forging process, Materials Science and Engineering: A. 845 (2022) 143260.
3. Nichul U., Hiwarkar V. Carbon dot complimentary green corrosion inhibitor for crystallographically textured Beta C titanium alloy for marine application: A state of art, Journal of Alloys and Compounds. 962 (2023) 171116.
4. Saurabh A., Meghana C.M., Singh P.K., Verma P.C. Titanium-based materials: synthesis, properties, and applications, Materials Today: Proceedings. 56 (2022) 412–419.
5. Pesode P., Barve S., Wankhede S. V., Jadhav D.R., Pawar S.K. Titanium alloy selection for biomedical application using weighted sum model methodology, Materials Today: Proceedings. 72 (2023) 724–728.
6. Ghosh M., Surekha S., Anisha M., Thirugnanam A. Ultra-fine grained commercial pure titanium for load-bearing applications, Materials Today: Proceedings. 80 (2023) 1534–1537.
7. J. Gummadi, S. Alanka, A review on titanium and titanium alloys with other metals for biomedical applications prepared by powder metallurgy techniques, Materials Today: Proceedings. (2023). in press
8. Han X., Ma J., Tian A., Wang Y., Li Y., Dong B., Tong X., Ma X. Surface modification techniques of titanium and titanium alloys for biomedical orthopaedics applications: A review, Colloids and Surfaces B: Biointerfaces. 227 (2023) 113339.
9. Ronoh K., Mwema F., Dabees S., Sobola D. Advances in sustainable grinding of different types of the titanium biomaterials for medical applications: A review, Biomedical Engineering Advances. 4 (2022) 100047.
10. Makurat-Kasprolewicz B., Ossowska A. Recent advances in electrochemically surface treated titanium and its alloys for biomedical applications: A review of anodic and plasma electrolytic oxidation methods, Materials Today Communications. 34 (2023) 105425.
11. Rogala-Wielgus D., Majkowska-Marzec B., Zieliński A., Jankiewicz B.J. Mechanical behavior of bi-layer and dispersion coatings composed of several nanostructures on ti substrate, Applied Sciences (Switzerland). 11 (2021).
12. Sunil B.R., Kranthi Kiran A.S., Ramakrishna S. Surface functionalized titanium with enhanced bioactivity and antimicrobial properties through surface engineering strategies for bone implant applications, Current Opinion in Biomedical Engineering. 23 (2022) 100398.
13. Zhou J.Z., Huang S., Zuo L.D., Meng X.K., Sheng J., Tian Q., Han Y.H., Zhu W.L. Effects of laser peening on residual stresses and fatigue crack growth properties of Ti-6Al-4V titanium alloy, Optics and Lasers in Engineering. 52 (2014) 189–194.
14. Dai F.Z., Geng J., Tan W.S., Ren X.D., Lu J.Z., Huang S. Friction and wear on laser textured Ti6Al4V surface subjected to laser shock peening with contacting foil, Optics and Laser
15. Petronić S., Čolić K., Đorđević B., Milovanović D., Burzić M., Vučetić F. Effect of laser shock peening with and without protective coating on the microstructure and mechanical properties of Ti-alloy, Optics and Lasers in Engineering. 129 (2020).

16. Lin Y., Yao J., Lei Y., Fu H., Wang L. Microstructure and properties of TiB2-TiB reinforced titanium matrix composite coating by laser cladding, Optics and Lasers in Engineering. 86 (2016) 216–227.
17. Akman E., Cerkezoglu E. Compositional and microscratch analyses of laser induced colored surface of titanium, Optics and Lasers in Engineering. 84 (2016) 37–43.
18. Zhu G., Xu Z., Jin Y., Chen X., Yang L., Xu J., Shan D., Chen Y., Guo B. Mechanism and application of laser cleaning: A review, Optics and Lasers in Engineering. 157 (2022) 107130.
19. Wang X., Zhang D., Gu C., Shen Z., Ma Y., Gu Y., Qiu T., Liu H. Micro scale laser shock forming of pure copper and titanium sheet with forming/blanking compound die, Optics and Lasers in Engineering. 67 (2015) 83–93.
20. Hua YU A., XU W., LU X., TAMADDON M., Wen LIU B., Wei TIAN S., ZHANG C., MUGHAL M.A., Zhen ZHANG J., Zong LIU C. Development and characterizations of graded porous titanium scaffolds via selective laser melting for orthopedics applications, Transactions of Nonferrous Metals Society of China (English Edition). 33 (2023) 1755–1767.
21. Convert L., Bourillot E., François M., Pocholle N., Baras F., Politano O., Costil S. Laser textured titanium surface characterization, Applied Surface Science. 586 (2022) 152807.
22. Simões I.G., Dos Reis A.C., Costa Valente M.L. Analysis of the influence of surface treatment by high-power laser irradiation on the surface properties of titanium dental implants: A systematic review, Journal of Prosthetic Dentistry. (2021) 1–8.
23. Souza J.C.M., Sordi M.B., Kanazawa M., Ravindran S., Henriques B., Silva F.S., Aparicio C., Cooper L.F. Nano-scale modification of titanium implant surfaces to enhance osseointegration, Acta Biomaterialia. 94 (2019) 112–131.
24. He W., Yao P., Chu D., Sun H., Lai Q., Wang Q., Wang P., Qu S., Huang C. Controllable hydrophilic titanium surface with micro-protrusion or microgroove processed by femtosecond laser direct writing, Optics and Laser Technology. 152 (2022) 108082.
25. Wedemeyer C., Jablonski H., Mumdzic-Zverotic A., Fietzek H., Mertens T., Hilken G., Krüger C., Wissmann A., Heep H., Schlepper R., Kauther M.D. Laser-induced nanostructures on titanium surfaces ensure osseointegration of implants in rabbit femora, Materialia. 6 (2019)
26. Yao H., Zou X., Zheng S., Hu Y., Zhang S., Liang C., Zhou H., Wang D., Wang H., Yang L., Li Q. Femtosecond laser-induced nanoporous layer for enhanced osteogenesis of titanium implants, Materials Science and Engineering C. 127 (2021) 112247.
27. Qiang Dou H., Liu H., Xu S., Chen Y., Miao X., Lü H., Jiang X. Influence of laser fluences and scan speeds on the morphologies and wetting properties of titanium alloy, Optik. 224 (2020).
28. Wang Y., Zhang M., Li V, Hu J. Study on the surface properties and biocompatibility of nanosecond laser patterned titanium alloy, Optics and Laser Technology. 139 (2021) 106987.
29. Pandey L.M. Design of biocompatible and self-antibacterial titanium surfaces for biomedical applications, Current Opinion in Biomedical Engineering. 25 (2022) 100423.
30. Kaur M., Singh K. Review on titanium and titanium based alloys as biomaterials for orthopaedic applications, Materials Science and Engineering C. 102 (2019) 844–862.
31. Abdal-hay A., Staples R., Alhazaa A., Fournier B., Al-Gawati M., Lee R.S., Ivanovski S. Fabrication of micropores on titanium implants using femtosecond laser technology: Perpendicular attachment of connective tissues as a pilot study, Optics and Laser Technology. 148 (2022) 107624.
32. Ushakov I., Simonov Y. Formation of surface properties of VT18u titanium alloy by laser pulse treatment, Materials Today: Proceedings. 19 (2019) 2051–2055.
33. Watanabe I., McBride M., Newton P., Kurtz K.S. Laser surface treatment to improve mechanical properties of cast titanium, Dental Materials. 25 (2009) 629–633.
34. Liu Q., Liu Y., Li X., Dong G. Pulse laser-induced cell-like texture on surface of titanium alloy for tribological properties improvement, Wear. 477 (2021) 203784.
35. Kümmel D., Linsler D., Schneider R., Schneider J. Surface engineering of a titanium alloy for tribological applications by nanosecond-pulsed laser, Tribology International. 150 (2020)
36. Lu J., Huang T., Liu Z., Zhang X., Xiao R. Long-term wettability of titanium surfaces by combined femtosecond laser micro/nano structuring and chemical treatments, Applied Surface Science. 459 (2018) 257–262.
37. Yu Z., Zhang J., Hu J. Study on surface properties of nanosecond laser textured plasma nitrided titanium alloy, Materials Today Communications. 31 (2022) 103746.
38. Katahira K., Ezura A., Ohkawa K., Komotori J., Ohmori H. Generation of bio-compatible titanium alloy surfaces by laser-induced wet treatment, CIRP Annals - Manufacturing Technology. 65 (2016) 237–240.
39. Calazans Neto J.V., Kreve S., Da C. Valente M.L., Reis A.C. Protein absorption on titanium surfaces treated with a high-power laser: A systematic review, Journal of Prosthetic Dentistry. (2022) 1–7.

40. Khoo L.K., Sakdajeyont W., Khanijou M., Seriwatanachai D., Kiattavorncharoen S., Pairuchvej V., Wongsirichat N. Titanium fixture implants treated by laser in dentistry: Review article, Journal of Oral and Maxillofacial Surgery, Medicine, and Pathology. 31 (2019) 381–385.
41. Papa S., Abou Khalil A., Hamzeh-Cognasse H., Thomas M., Maalouf M., Di Maio Y., Sedao X., Guignandon A., Dumas V. Dual-functionalized titanium by ultrafast laser texturing to enhance human gingival fibroblasts adhesion and minimize Porphyromonas gingivalis colonization, Applied Surface Science. 606 (2022) 154784.
42. Shirazi H.A., Chan C.W., Lee S. Elastic-plastic properties of titanium and its alloys modified by fibre laser surface nitriding for orthopaedic implant applications, Journal of the Mechanical Behavior of Biomedical Materials. 124 (2021) 104802.
43. Jażdżewska M., Bartmański M., Zieliński M., Kwidzińska D.B. Effect of Laser Treatment on Intrinsic Mechanical Stresses in Titanium and Some of Its Alloys, Applied Sciences (Switzerland). 13 (2023).
44. Jażdżewska M., Kwidzińska D.B., Seyda W.,Fydrych D., Zieliński A. Mechanical Properties and Residual Stress Measurements of Grade IV Titanium and Ti-6Al-4V and Ti-13Nb-13Zr Titanium Alloys after Laser Treatment, Materials. 14 (2021) 6316.
45. Lee Y.H., Kwon D. Residual stresses in DLC/Si and Au/Si systems: Application of a stress-relaxation model to the nanoindentation technique, Journal of Materials Research. 17 (2002) 901–906.
46. Majumdar P., Singh S.B., Chakraborty M. Wear response of heat-treated Ti-13Zr-13Nb alloy in dry condition and simulated body fluid, Wear. 264 (2008) 1015–1025.
47. Simões I.G., Dos Reis A.C., Costa Valente M.L. Analysis of the influence of surface treatment by high-power laser irradiation on the surface properties of titanium dental implants: A systematic review, Journal of Prosthetic Dentistry. 129 (2023) 863–870.
48. Kosturkiewicz Z., Metody krystalografii, Wydawnictwo Poznań, 2004.
49. Yang L., Ding X., Zhou Y. Femtosecond laser induced periodic nanostructures towards enhanced anti-corrosive property of titanium, Surface and Coatings Technology. 463 (2023) 129533.
50. Xue A., Lin X., Wang L., Lu X., Ding H., Huang W.Heat-affected coarsening of β grain in titanium alloy during laser directed energy deposition, Scripta Materialia. 205 (2021) 114180.
51. Li Z., Li Y., Liu S., Wu L., Qin W., Wu X. Enhancement of oxidation resistance of Cr/CrN composite coating on Zr-4 surface by high lattice-matched interfacial Engineering, Journal of Nuclear Materials. 574 (2023).
52. Zhang H., Cai Z., Chi J., Sun R., Che Z., Zhang H., Guo W. Fatigue crack growth in residual stress fields of laser shock peened Ti6Al4V titanium alloy, Journal of Alloys and Compounds. 887 (2021) 161427.
53. Yang J., Tang H., Wei P., Gao H., Wang J., Huo H., Zhu Y. Microstructure and Mechanical Properties of an Ultrahigh-strength Titanium alloy Ti-4.5Al-5Mo-5V-6Cr-1Nb Prepared Using Laser Directed Energy Deposition and Forging: A Comparative Study, Chinese Journal of Mechanical Engineering: Additive Manufacturing Frontiers. 2 (2023) 100064.
54. Chauhan A.S., Jha J.S., Telrandhe S., S. V, Gokhale A.A., Mishra S.K. Laser surface treatment of α-β titanium alloy to develop a β -rich phase with very high hardness, Journal of Materials Processing Technology. 288 (2021) 116873.
55. Costa F.H., Sallica-Leva E., Mello M.G., Amigó V,. Caram R, Fogagnolo J.B. Stiffness and hardness gradients obtained by laser surface treatment of aged β-Ti alloys: The role of ω phase, Surface and Coatings Technology. 467 (2023).
56. Hua Y., Guo B., Jiang L., Chen R., Zhang T., Chen M. Strengthened and hydrophobic surface of titanium alloy by femtosecond laser shock peening without a protective or sacrificial layer, Optics and Laser Technology. 167 (2023) 109787.
57. Lisiecki, A., & Kurc-Lisiecka, A. (2023). Laser Cladding of NiCrBSi/WC+ W2C CompositeCoatings. Coatings, 13(3), 576.
58. Kadyroldina, A., Alontseva, D., Voinarovych, S., Łatka, L., Kyslytsia, O., Azamatov, B., ... & Burburska, S. (2022). Microplasma spraying of hydroxyapatite coatings on additive manufacturing titanium implants with trabecular structures. Materials Science-Poland, 40(4), 28-42.
59. Tuz, L., Sokołowski, Ł., & Stano, S. (2023). Effect of Post-Weld Heat Treatment on Microstructure and Hardness of Laser Beam Welded 17-4 PH Stainless Steel. Materials, 16(4), 1334.